

PV Solar Farm Control as STATCOM (PV-STATCOM) for Alleviating Subsynchronous Oscillations

R. Salehi and R. K. Varma
Smart PV Inverter and FACTS Laboratory
The University of Western Ontario
London, ON, Canada

SUMMARY

This paper presents a novel concept of controlling PV solar farm as STATCOM, termed PV-STATCOM, to mitigate subsynchronous oscillations (SSO) in a synchronous generator (SG) connected to a series capacitive compensated transmission line.

A modified IEEE First SSR Benchmark system with integrated PV solar farm and a realistic series compensation level is adopted to demonstrate the ability of PV-STATCOM in alleviating SSO. The PV system maybe located at either SG terminal or remotely from the SG. SG speed in former case and line active power in latter case are employed as the control signal for subsynchronous damping controller.

At daytime, once SSO instability occurs in the system, the PV solar farm stops its conventional active power generation and makes the entire capacity of its inverter available to operate in Full-STATCOM mode and damp SSO. When SSO is damped, the PV solar farm comes back to its normal active power generation in a ramped manner to avoid recurrence of oscillations. During active power ramp-up the subsynchronous damping controller uses the remaining capacity of the solar inverter and operates in Partial-STATCOM mode to prevent the recurrence of SSO and achieve fast ramp-up. At nighttime, the solar inverter is idle, and its entire capacity is used as STATCOM to damp SSO.

PV-STATCOM can thus offer 24/7 SSO damping service to the power system. Results of modal analysis and electromagnetic transients' studies validate the effectiveness of PV-STATCOM for alleviation SSO in SG. This novel method of utilizing existing PV system as PV-STATCOM to alleviate SSO can obviate the need of installing expensive FACTS devices such as STATCOM or SVC to achieve this objective.

KEYWORDS

PV system, Modelling, System control and operation, Sub Synchronous Resonance (SSR), Series compensation, PV-STATCOM, Smart inverter

1. INTRODUCTION

Series capacitive compensation is widely used to increase power transfer limit of existing transmission lines as it is economical and simple. But, it causes subsynchronous oscillations (SSO) in the power system which can potentially lead to subsynchronous resonance (SSR) if not controlled.

SSR is an unstable phenomenon in the power system that can lead to significant monetary losses to the utility [1]. SSR caused shaft failure in steam turbine synchronous generator of Mohave power plant, USA, two times in 1970 and 1971 [1]. Damages in series capacitor of the transmission line and Type-III wind farm due to undamped SSO has been reported in Texas, USA, in 2009 [2]. SSR also was reported due to adverse interaction between HVDC system and turbine generator in North Dakota, USA, in 1980 [3]. Utilizing Flexible AC Transmission System (FACTS) devices for SSR damping have been proposed and studied in many papers, such as Static Var Compensator (SVC) [4], Static Synchronous Compensator (STATCOM) [5], Thyristor Controlled Series Capacitor (TCSC) [6], and Gate-Controlled Series Capacitor (GCSC) [6].

Nowadays, many large-scale PV solar farms rated over 100 MW are both commissioned and planned to operate around the world such as: Tengger Desert Solar Park (1500 MW) in China, Yanchi Solar PV Station (1000 MW) in china, Kurnool Ultra Mega Solar Park (1000 MW) in India, Longyangxia Dam Solar Park (850 MW) in China, Kamuthi Solar Power Project (648 MW) in India, Solar Star I and II (579 MW) in USA, Desert Sunlight Solar Farm and Topaz Solar Farm (550 MW each) in USA [7]. Most of these PV solar farms are located far from load center and likely connected to transmission lines which may have series capacitive compensation. For example, Agua Caliente Solar farm (290 MW) in Arizona, USA is connected to Hassayampa-North Gila 500 kV transmission line which is a series compensated transmission line [8].

A new control of PV solar farm as STATCOM, termed PV-STATCOM, has been presented in [9, 10]. In [10], PV-STATCOM is employed to mitigate SSR in synchronous generator (SG) connected to a series compensated transmission line when PV solar farm is located at SG bus. At day time, once undamped SSO detected, the PV system stops its active power generation (P_{PV}), and the entire capacity of the inverter is used to function as STATCOM and mitigate SSR. PV solar farm returns to its normal operation after SSR mitigation. PV inverter is idle at night, so its capacity is completely used as STATCOM for SSR alleviation. However in [10], the efficacy of PV-STATCOM in alleviating SSO in SG has been studied just through electromagnetic transient studies and only for one location of PV Solar farm.

This paper studies the effectiveness of PV-STATCOM for SSO mitigation in SG through modal analysis and electromagnetic transient studies using MATLAB/Simulink software. A modified IEEE First SSR Benchmark system [11] with integrated PV solar farm and a realistic compensation level is employed to study the proposed method. The studies have been done for two different locations of PV solar farm: 1) SG bus, and 2) line midpoint. Generator speed (ω_r) is used as the input control signal when PV solar farm is connected to SG bus. However a local signal, line active power flow (P_{Line}), is used as control signal when PV solar farm is located at line midpoint. By using local signal as control signal, not only communication delay is avoided but also the PV-STATCOM alleviation service becomes independent of PV solar farm location.

The rest of the paper is organized as follows. Section 2 explains the concept of PV-STATCOM controller. The study system is described in Section 3. The control system of PV-STATCOM is explained in Section 4. Section 5 consists of the simulation results to validate the effectiveness of PV-STATCOM in damping SSO. Section 6 concludes the paper.

2. CONTROL CONCEPT OF PV-STATCOM

Fig. 1 shows the typical pattern of active and reactive power capacity of a PV inverter on a sunny day. The PV-STATCOM has two modes of operation: 1) Full-STATCOM, and 2) Partial-STATCOM [10].

In Full-STATCOM mode, reactive power exchange is the priority and the entire capacity of solar inverter is utilized for dynamic reactive power control as a STATCOM. During daytime, when growing SSO is detected in the system, PV-STATCOM controller ceases active power generation by the PV solar farm and makes the entire capacity of solar inverter available to operate as STATCOM. After SSO instability mitigation, the PV system restores its power output P_{PV} to its pre-fault level in a ramped manner. Based on grid codes [12], [13], [14], a gradual increment of P_{PV} is required to prevent initiation of low frequency oscillation in the system. At nighttime, the solar panels do not generate active power and the PV inverter can completely operate as STATCOM. Therefore, PV-STATCOM provides SSO alleviation service to the system on a 24/7 basis.

In Partial-STATCOM mode, the remaining capacity of PV inverter after active power generation at daytime is used for dynamic reactive power control as a STATCOM for SSO alleviation. The active power generation is the priority in this mode. During the ramp-up of P_{PV} after SSR alleviation, PV-STATCOM utilizes the unused capacity of VSI and operates in Partial-STATCOM mode to avoid the recurrence of SSO and achieve fast ramp-up. This is a novel functionality during the power ramp-up proposed in this paper, which is not specified in existing grid codes.

3. STUDY SYSTEM

The study system shown in Fig. 1 is a modified IEEE First SSR Benchmark system [11] augmented with a 300-MW PV solar farm which may be connected either at SG bus (Bus A) or at line midpoint (Bus C). The SG and PV solar farm are connected to the infinite bus through a series capacitive compensated transmission line. In this paper, the 892-MW SG operates at 500 MW, PV solar farm operates at its rated power (300 MW), and a realistic compensation level (k) of 50% is considered for SSO mitigation studies. The entire system is modeled in MATLAB/Simulink software. To represent the dynamics of mechanical system, an aggregated six-mass turbine is considered, while the mechanical damping is assumed to be zero in this study to study the worst case damping situation. The PV panels are represented by a controlled current source as a dc source which follows the I-V characteristic of PV panels. This dc source is connected to a voltage source inverter (VSI) which is linked to transmission line through a filter and a coupling transformer.

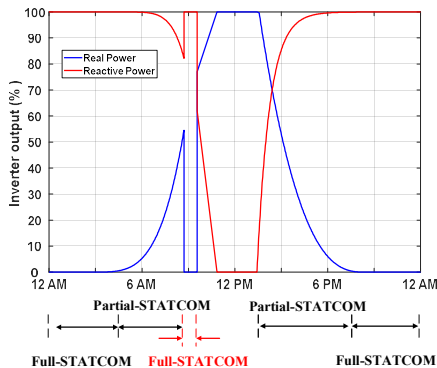


Fig.1. PV inverter output for 24 hours duration [10].

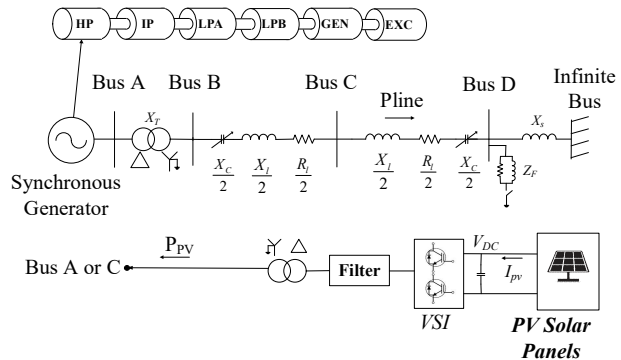


Fig.2. Study system: modified IEE First SSR Benchmark system with integrated PV solar farm

4. CONTROL SYSTEM

The PV inverter control is based on the dq -reference frame model of VSI [15]. The voltage vector is aligned with the quadrature axis and V_d equals zero in this paper. Therefore, the d -axis control loop controls the reactive power of the VSI and the q -axis control loop controls the active power of the VSI. The current controller regulates the output current of VSI by providing appropriate modulation indexes m_d and m_q , as explained in [15].

4.1 Subsynchronous Damping Controller (SSDC)

As shown in Fig. 3 (a), The subsynchronous damping controller (SSDC) consists of a filter block, a controller gain block, a phase compensator (lead-lag compensator) and a limiter block. When PV solar farm is connected to SG bus, ω_r is employed as control signal for the SSDC. In this case, the washout filter is used as the filter to remove the dc part of ω_r and obtain its deviation ($\Delta\omega_r$). However, P_{Line} is utilized as control signal for the SSDC when PV system is connected to the middle of the line. This avoids the communication delay if ω_r were to be chosen as control signal. In this case, a band-pass filter is used as the filter to extract the subsynchronous frequency components of P_{Line} . The output of the filter which includes subsynchronous component of control signal is amplified with the controller gain. Then it is passes through phase compensator to provide i_{dref} for the current controller. The SSDC mitigates SSO in the system by generating appropriate i_{dref} and consequently reactive power output of PV solar farm (Q_{PV}).

4.2 DC Voltage Controller

The DC voltage controller, as shown in Fig. 3 (b), includes a power point tracking (PPT) block, and a PI controller. The PPT block controls P_{PV} by producing reference dc voltage (V_{DC-ref}). In normal operation, PV solar farm performs in its conventional unity power factor mode and the PPT block sets the dc side voltage (V_{op}) to the maximum power point (MPP) voltage (V_{MP}) at which maximum active power is extracted from the solar panels. The error between V_{DC-ref} and measured voltage of dc bus (V_{DC}) passes through the PI controller to provide I_{qref} for the current controller, and consequently control P_{PV} .

The DC voltage controller constantly monitors the deviation of control signal (Δx). Once any fault or disturbance occurs in the system, the PPT system increases V_{DC-ref} to the open circuit voltage of PV panels (V_{OC}) and makes $P_{PV}=0$. Therefore, the entire capacity of PV inverter is available to be used by SSDC and operate in Full-STATCOM mode. After SSR mitigation, The PPT block brings PV solar farm back to its conventional active power generation gradually. In order to do this, the V_{DC-ref} is decreased from V_{OC} to V_{MP} in a ramped manner. By using the remaining capacity of VSI during the increment of P_{PV} , the PV-STATCOM controller operates in Partial-STATCOM mode to prevent recurrence of SSO and achieve fast ramp-up.

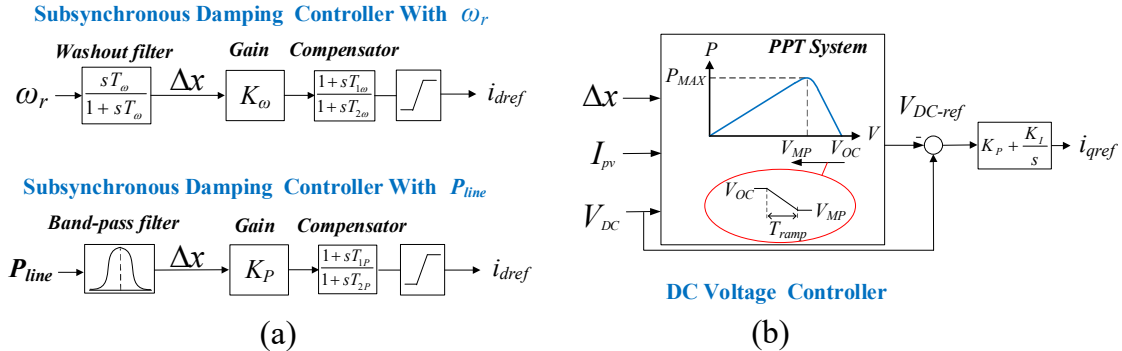


Fig.3. (a) Subsynchronous damping Controller. (b) DC Voltage Controller.

The MATLAB optimization block, genetic algorithm (GA), is used to determine the controller parameters. An objective function (OF) is defined to accomplish maximum damping for the system. In (1), ζ_j is the damping ratio of j^{th} eigenvalue of the system. This OF ensures that the eigenvalues of the system have positive damping ratio.

$$OF = \sum_{j=1}^n (1 - |\zeta_j|) \quad , \quad \zeta_j > 0 \quad (1)$$

5. EIGENVALUE ANALYSIS and TRANSIENT SIMULATION

The system under study is modeled in MATLAB/Simulink software while 892-MW SG generates 500 MW, P_{PV} is 300 MW, and k is considered 50%. The linearization toolbox of MATLAB software is utilized for small signal analysis of system. Electromagnetic transient studies are carried out for a three phase to ground fault at $t=5$ sec for 5 cycles at bus D.

5.1 PV solar farm located at SG terminal

In this section, the effectiveness of PV-STATCOM SSO alleviation is studied when PV solar farm is connected at SG terminal. The eigenvalues of the system with and without the proposed controller are shown in Table 1. This table includes torsional Modes 0 to 5, and network modes (subsynchronous and super synchronous). It is seen that without PV-STATCOM controller, torsional Mode 2 has positive real part and is unstable. It should be noted that without PV-STATCOM controller, the frequency of subsynchronous mode is close to the frequency of Mode 2, and the interaction between them causes instability in Mode 2. However with SSDC, the damping of torsional Modes 1 to 4 increases noticeably. Also, the damping of subsynchronous mode is slightly decreased, while damping of Mode 0 and super synchronous mode is marginally enhanced. This eigenvalue study clearly demonstrates the effectiveness of the proposed PV-STATCOM controller with SSDC in alleviation of SSO.

Table 1 Eigenvalues of system while PV located at SG bus, and $k=50\%$.

Modes	Without PV-STATCOM	With PV-STATCOM
0	-1.185± 10.81 i	-1.39±9.981 i
1	-0.144± 99.89i	-1.232± 96.74i
2	0.085± 127.24i	-0.129±126.27 i
3	-0.232± 160.29i	-1.01±163.49 i
4	-0.057± 202.83i	-0.56±205.25 i
5	-0.28± 298.17i	-0.25± 298.18i
Network-1(Sub)	-1.918±137.78 i	-1.544±141.26 i
Network-2(Super)	-5.5± 616.53i	-5.69±614.97 i

Figs. 4 (a)-(b) illustrate voltage at SG terminal (V_S), and SG rotor speed (ω_r), respectively, when PV-STATCOM controller is not implemented in PV system. The growing SSO in V_S and ω_r show the instability of the system and corroborate the results of eigenvalue study.

Figs. 5 (a)-(d) depict voltage at SG terminal (V_S), SG rotor speed (ω_r), torque between HP-IP (T_{HI}), and torque between LPA-LPB (T_{AB}), respectively, with PV-STATCOM controller. These figures show the effectiveness of PV-STATCOM in SSO mitigation and validate the eigen-analysis results of Table 1.

Figs. 6 (a)-(d) depict PV system variables including active power of PV system (P_{PV}), reactive power of PV system (Q_{PV}), dc side voltage (V_{DC}), and dc side current (I_{DC}), respectively. As shown in Fig. 6 (a), before fault occurrence, PV solar farm operates in its conventional mode and extracts maximum power from PV panels ($P_{PV}=300$ MW). Once fault occurs and SSO detected by PV-STATCOM controller, the DC voltage controller increases V_{op} to V_{OC} (Fig. 6

(c). Consequently, I_{DC} and P_{PV} go to zero with slight delay based on the controller time constant. The VSI is now entirely available to operate in Full-SATTCOM mode. Once the SSO in ω_r are damped to within 1 rad/sec at $t=7.92$ sec, PV solar farm restores P_{PV} gradually. To achieve this, DC voltage controller increases V_{op} from V_{OC} to V_{MP} in 5 seconds in ramped manner. During P_{PV} ramp-up, the remaining capacity of VSI is used by SSDC in Partial-STATCOM mode to prevent the SSO recurrence and fast ramp-up. It can be seen in Fig. 6 (b) that the maximum Q_{PV} needed to damp SSR in this case is 174 Mvar.

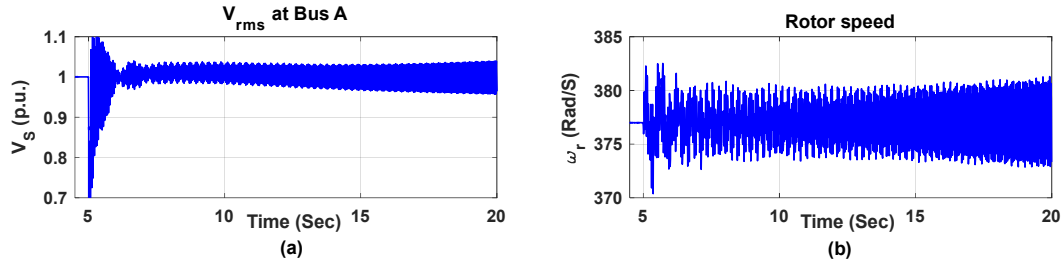


Fig.4. System response, PV located at SG bus, without PV-STATCOM controller, $k=50\%$.

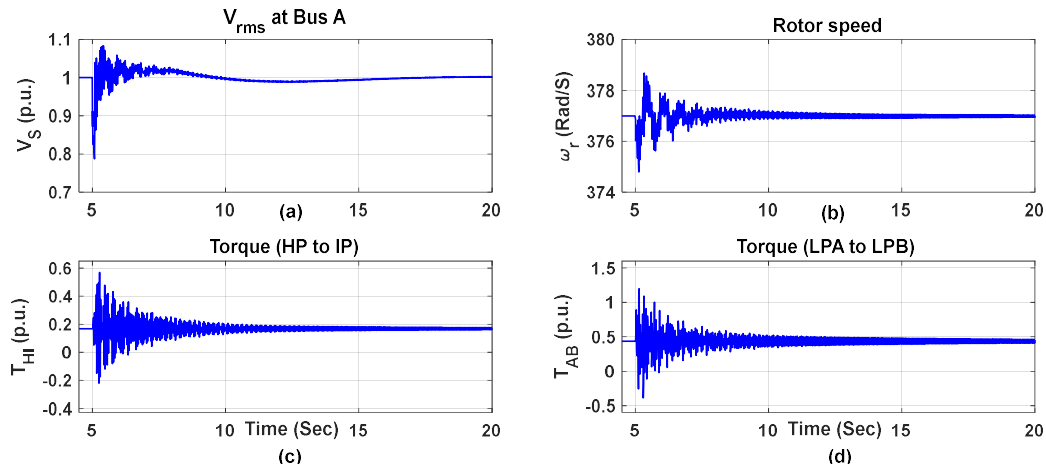


Fig.5. System response, PV located at SG bus, with PV-STATCOM controller, $k=50\%$

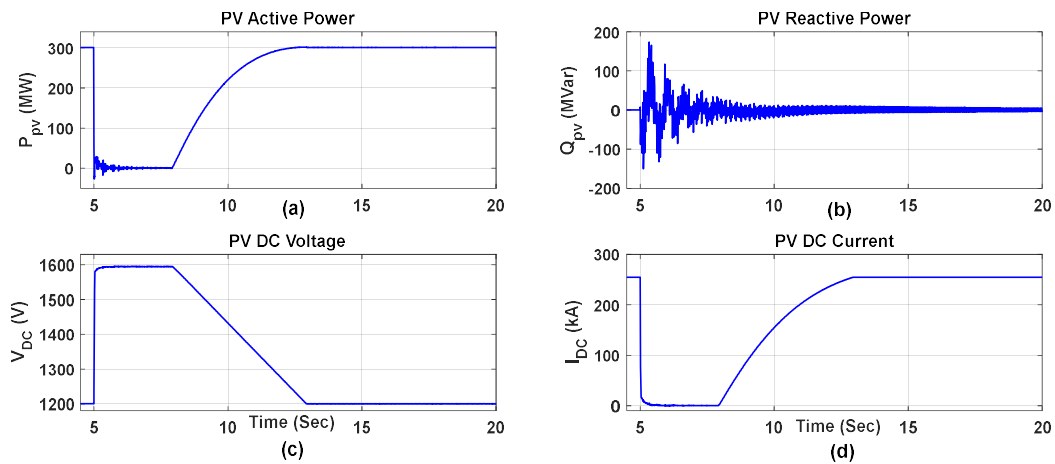


Fig.6. PV Solar farm response, PV located at SG bus, with PV-STATCOM controller, $k=50\%$

5.2 PV solar farm located at line midpoint

In this section, the effectiveness of PV-STATCOM in damping SSO while PV solar farm is connected to line midpoint, is investigated. Table 2 shows the eigenvalues of the system with and without PV-STATCOM controller. Eigenvalues of the system without PV-STATCOM controller show that the system has an unstable mode (Mode 2), similar to previous case (Table 1). However, it is seen that implementation of PV-STATCOM controller moves Mode 2 to left half plane and makes it stable. The damping of subsynchronous mode is also improved. However, the PV-STATCOM does not have a noticeable effect on other modes. In this case, the SSDC uses P_{Line} as control signal and utilizes a band-pass filter which extracts the subsynchronous components of P_{Line} . Therefore, subsynchronous damping controller has more influence on subsynchronous mode and Mode 2, whose frequencies are close to each other.

Table 2 Eigenvalues of system while PV located at line midpoint, and $k=50\%$.

Modes	Without PV-STATCOM	With PV-STATCOM
0	$-1.25 \pm 11.068i$	$-1.25 \pm 11.067i$
1	$-0.085 \pm 99.93i$	$-0.093 \pm 99.91i$
2	$0.132 \pm 127.24i$	$-0.14 \pm 128.83i$
3	$-0.224 \pm 160.27i$	$-0.226 \pm 160.28i$
4	$-0.05 \pm 202.81i$	$-0.051 \pm 202.82i$
5	$-0.28 \pm 298.17i$	$-0.28 \pm 298.17i$
Network-1(Sub)	$-2.799 \pm 137.81i$	$-3.45 \pm 135.17i$
Network-2(Super)	$-5.55 \pm 616.48i$	$-5.53 \pm 616.55i$

Figs. 7 (a)-(d) depict active power flow of the line (P_{Line}), SG rotor speed (ω_r), dc side voltage (V_{DC}), and reactive power of PV system (Q_{PV}), respectively, while PV solar farm augmented with PV-STATCOM controller is located at line midpoint. Once fault occurs in the system, PV-STATCOM controller increases the dc side voltage to V_{OC} and makes $P_{PV}=0$. The P_{Line} consequently reduces. SSDC uses VSI in Full-STATCOM mode and mitigates SSO. Fig. 7 (b) shows that PV-STATCOM successfully damps torsional SSO in the SG rotor speed. Once SSO is mitigated at $t=9.21s$, the DC voltage controller restores P_{PV} by decreasing dc voltage gradually to its pre-fault condition. As explained in previous section, PV-STATCOM operates in Partial-STATCOM mode during ramp-up. The Q_{PV} required to damp SSO instability in this case is 188 Mvar.

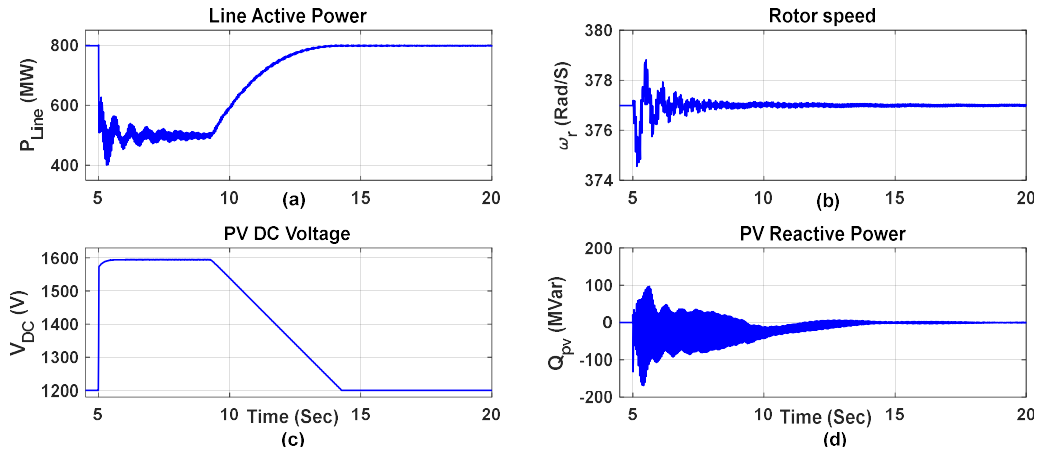


Fig.7. System response, PV located at line midpoint, with PV-STATCOM controller, $k=50\%$

6. CONCLUSION

In this paper, a novel concept of using PV solar farm as STATCOM is demonstrated to mitigate SSO in a synchronous generator. A modified IEEE First SSR Benchmark system with an integrated PV solar farm is employed to study the effectiveness of PV-STATCOM SSO damping. Studies are performed for a realistic series compensation level, $k=50\%$, and two different locations of PV solar farm: 1) SG bus, and 2) line midpoint. The SG rotor speed (ω_r) is used as control signal for subsynchronous damping controller when PV is connected at SG bus. To prevent communication delay, the subsynchronous damping controller uses the active power flow (P_{Line}) as input signal when PV system is located at line midpoint.

Eigenvalue studies of the system show that implementation of PV-STATCOM controller in PV system successfully improves the damping of the unstable mode and makes it stable.

It is noted that subsynchronous damping controller affects all the torsional modes when it uses ω_r as input signal. However, with P_{Line} as control signal, it mostly influences the SSO mode and related torsional mode and does not influence other modes noticeably.

The time domain results validate the effectiveness of PV-STATCOM in damping SSO. It is noted that PV-STATCOM needs slightly more reactive power and time to alleviate SSO when PV system is located to line midpoint.

The entire process of SSO instability alleviation from fault occurrence till restoration of PV solar farm to its pre-fault condition takes place in less than half a minute. This application of existing PV solar farm as PV-STATCOM to damp SSO can obviate the need of installing expensive FACTS devices such as STATCOM or SVC.

BIBLIOGRAPHY

- [1] IEEE Committee Report, "Reader's guide to subsynchronous resonance," *IEEE Trans. on Power Systems*, vol. 7, pp. 150-157, 1992.
- [2] A. E. Leon and J. A. Solsona, "Sub-Synchronous Interaction Damping Control for DFIG Wind Turbines," *IEEE Transactions on Power Systems*, vol. 30, pp. 419-428, 2015.
- [3] K. Mortensen, E. V. Larsen, and R. J. Piwko, "Field Tests and Analysis of Torsional Interaction Between the Coal Creek Turbine-Generators and the CU HVdc System," *IEEE Trans. Power Apparatus and Systems*, vol. PAS-100, pp. 336-344, 1981.
- [4] A. E. Hammad and M. El-Sadek, "Application of a Thyristor Controlled Var Compensator for Damping Subsynchronous Oscillations in Power Systems," *IEEE Trans. Power Apparatus and Systems*, 1984.
- [5] M. S. El-Moursi, B. Bak-Jensen, and M. H. Abdel-Rahman, "Novel STATCOM Controller for Mitigating SSR and Damping Power System Oscillations in a Series Compensated Wind Park," *IEEE Transactions on Power Electronics*, vol. 25, pp. 429-441, 2010.
- [6] H. A. Mohammadpour, M. M. Islam, E. Santi, and Y. J. Shin, "SSR Damping in Fixed-Speed Wind Farms Using Series FACTS Controllers," *IEEE Trans. on Power Delivery*, vol. 31, pp. 76-86, 2016.
- [7] *PV Resources, Large scale photovoltaic power plants ranking 1-50*. [Online]. Available: <http://www.pvresources.com/en/pvpowerplants/top50pv.php#notes>
- [8] *First Solar, Projects, Agua Caliente Solar Project*. [Online]. Available: <http://www.firstsolar.com/Resources/Projects/Agua-Caliente-Solar-Project>
- [9] R. K. Varma, "Multivariable Modulator Controller for Power Generation Facility," U.S. Provisional Patent Patent, PCT Application (PCT/CA2014/051174) filed on December 6, 2014.
- [10] R. K. Varma and R. Salehi, "SSR Mitigation With a New Control of PV Solar Farm as STATCOM (PV-STATCOM)," *IEEE Trans. on Sustainable Energy*, vol. PP, pp. 1473-1483, 2017.
- [11] IEEE Subsynchronous Resonance Task Force, "First benchmark model for computer simulation of subsynchronous resonance," *IEEE Trans. Power Apparatus and Systems*, vol. 96, pp. 1565-1572, 1977.
- [12] BDEW: 'Technical Guideline: Generating Plants Connected to the Medium Voltage Network', 2008
- [13] IEEE Std 1547: 'IEEE Standard for Interconnection and Interoperability of Distributed Energy Resources with Associated Electric Power Systems Interfaces', 2018
- [14] 'Reliability Standards for the Bulk Electric Systems of North America', <http://www.nerc.com/pa/Stand/Reliability%20Standards%20Complete%20Set/RSCompleteSet.pdf>, accessed 15 May 2018
- [15] A. Yazdani and R. Iravani, *Voltage-sourced converters in power systems: modeling, control, and applications*: John Wiley & Sons, 2010.